Int. J. Electrochem. Sci., 11 **(2016)** 7370 – 7379, doi: 10.20964/2016.09.41

International Journal of ELECTROCHEMICAL SCIENCE
www.electrochemsci.org

Short Communication

Porphyrin Functionalized Graphene for Sensitive Electrochemical Detection of Uric Acid

Yun Yang[1,2,*], *Ruirui Sun*[1], *Mingxiang Li*[1], *Boya Geng*[1], *Jingyi Deng*[1] *and, Mingyi Tang*[1]

[1] Department of Application Chemistry, College of Science, Tianjin University of Commerce, Tianjin, 300134, P.R . China;
[2] Tianjin Key Laboratory for Prevention and Control of Occupational and Environmental Hazards, Logistics University of PAPF Tianjin, 300162, P.R . China.
[*]E-mail: yyun@tjcu.edu.cn

Received: 10 June 2016 / *Accepted:* 13 July 2016 / *Published:* 7 August 2016

In this study, by employing nanobiocomposite from porphyrin modified graphene oxide, we make a stable and sensitive amperometric UA amperometric biosensor. An easy wet-chemical way for synthesizing porphyrin–graphene oxide hybrid nanosheets (T–GOs) was used. Different kinds of ways, including electrochemistry and transmission electron microscopy (TEM), have been used to present how the TPPC–GOs form. Between porphyrin and graphene oxide, there was the synergistic effect. Therefore, the nanosheets greatly performed to the detention of uric acid (UA). Incorporating the porphyrin onto graphene oxide surface caused over doubled increasement of the amperometric reaction to UA of the porphyrin improved electrode. At 0.25 V, UA has been checked successfully. The reaction indicates a great linear range from 0.02 to 5 mM with detection limit 1 μM. Applied in urine UA and blood, the improved electrode performed well.

Keywords: Electrochemistry; Uric acid; Porphyrin; Graphene oxide.

1. INTRODUCTION

In human metabolism, endogenous purine derivatives produce the main end product ---the uric acid (UA). In body fluid, the alteration of UA concentration may lead to some pathological problems, such as neurological diseases, neurological diseases, gouty arthritis and cardiovascular [1-3]**Error! Bookmark not defined.**. On the purpose of understanding the clinical result of the change of UA concentration, a useful and easy method is very important for the daily UA detection. Because of its briefness, strong sensitivity, and suitability for miniaturization, in biological media, electrochemistry may be useful for the UA examination [4-9]. Nevertheless, interferential species generally have impact on the UA electrochemical oxidation [10, 11].

On the purpose of avoiding such kind of selective problem, some methods recorded are applying chemically and physically-modified electrodes. Nanomaterials are cheap, steadier to biodegradation, easy to access, and not easy to denaturation. Therefore, in constructing biosensors, the appearance and updated development of nanotechnology and nanoscience provides new opportunities to applying nanomaterials [12]. Graphene is a new two-dimensional (2D) structure, which is made of sp^2-hybridized carbon. For graphitic materials of all other dimensionalities, graphene is regarded as a fundamental building block. Graphene is a kind of ‘‘rising star’’ material, because of its different kinds of electrical properties, wonderful thermal, mechanical and special nanostructure, which has obtained numerous attention from scientific communities experimentally and theoretically [13-15]. Various functionalities or extra molecules are used to modify grapheme to realize more helpful properties.

Porphyrins are called ‘the pigments of life’. In the visible-light area, porphyrins have a very high extinction coefficient. They possess promising photochemical ability of transferring electrons. Moreover, their structures are predictably rigid [16]. The porphyrin-modified acceptor nanoparticles and porphyrins present great optoelectronic properties [17]. As a famous functional dye, for obtaining new optoelectronic properties, derivatives of porphyrin have been employed to modify carbon nanotubes [18]. Lately, a kind of graphene hybrid material that covalently functionalized with porphyrin has been presented wonderful property of optical limitation and compounded[19, 20]. Hence, through the way of connecting optoelectronically active porphyrin moleculesand two-dimensional graphene nanomaterials, for optical and/ or optoelectronic, multipurpose nanometer-scale materials would be expected to be created.

Actually, in the explosive nitroaromatic mixture, the interaction of porphyrin-nitroaromatic mixture has been broadly employed for fluorescent detection. [21, 22]. Through the way of connecting the explosives of powerful affinity and advantage of porphyrin, and graphene of good capability of charge transfer and big ratio of surface to volume, for the electrochemical detection of ultratrace explosives, porphyrin functionalized grapheme with good sensitivity, may be a great choice.

2. EXPERIMENTAL

2.1. Reagents

Graphite was bought from Sinopharm Chemical Reagent Co. Porphyrin 5, 10, 15, 20-Tetra (4-pyridyl)-21H, 23H-porphine (TCPP) were obtained from Logan, UT. Sodium hydrogen phosphate, potassium ferricyanide, potassium ferrocyanide and dopamine were got from Sigma–Aldrich. As for Uric acid and ascorbic acid, they were bought from Alfa Asear and China Beijing Chemicals Inc. supply ammonia solution of 25 wt% and hydrazine solution of 85%. Ultra-pure water (18.2 M cm, Milli-Q, Millipore) was employed to make preparation for the whole aqueous solutions.

2.2. Preparations of Graphene Oxide

An improved Hummers method employed $KMnO_4$, H_2SO_4 and $NaNO_3$ to synthesize graphite oxide from natural graphite [23]. 10% HCl solution was used to wash the oxidized material. Then, the

oxidized material was rinsed with several amounts of Milli-Q water, and vacuum was used for filtering it. After these steps, the oxidized material was purified. To obtain 2 mg/mL concentration, after sonicating in ambient condition for 60 min, as-prepared oxidized material was dissolved in distilled water to prepare graphene oxide.

2.3. Preparations of Graphene and Porphyrin Functionalized Graphene

In the as-prepared graphene oxide aqueous dispersion, N,N-Dimethylformamide (DMF) was put, and the volume ratio of DMF to H_2O is 9. An even dispersion of the graphene oxide was obtained at concentration is 0.2 mg/mL. At 80 ^oC, dispersion was heated, into which, hydrazine monohydrate with the weight ratio of graphene oxide to hydrazine = 2:1 was put. After 12 hours, the mixture produced a kind of black graphene dispersion. And then, the graphene dispersion was put into DMF. For the preparation of porphyrin functionalized graphene, adequate TCPP solution (10 mM in DMF) was dropwise put into the graphene dispersion. At room temperature, stirring mixture solution lasted for 6 h. By five washing cycles, extra porphyrin was got rid off, included solid resuspension in DMF, filtration (discarding the filtrate) and sonication. In the end, in DMF, porphyrinmodified grapheme concentration is 0.05 mg/mL approximately (denoted as TPCC/RGO).

2.4. Apparatus and characterization

FEI TECNAI G2 20 high-resolution transmission electron microscope operating at 200 kV was employed to record the images of sample.

2.5. Electrochemical measurements

First of all, a piece of diamond paper and 0.05 m alumina slurry were used to polish the bare GCE to a mirror finish. Secondly, in ethanol and water, bare GCE went through ultrasonic cleaning for 2min separately. Thirdly, high-purity nitrogen steam was employed to dry GCE for the further modification. Fourthly, on the GCE surface, GNs-based nanocomposites dispersion (2 μL) was dropped. Fifthly, the GCE was put under an infrared lamp for drying. Finally, the modified electrodes were successfully got. The electrochemical detection of uric acid was conducted by a three electrode system, which a 3M Ag/AgCl and a Pt foil were applied as a reference electrode and counter electrode, respectively. The electrode surface electron transfer performance was evaluated by the electrochemical impedance spectroscopy (EIS). 5 mM $[Fe(CN)_6]^{3-/4-}$ and 0.1 M KCl were used as probe and supporting electrolyte, respectively. 10^1 to 10^5 Hz was selected as detection frequency range. 5 mV was selected as the amplitude value. Quantitative determination of uric acid was using amperimetric method at 0.1M PBS (pH = 7) with fitting potential of 0.25 V.

3. RESULT AND DISCUSSION

3.1. Materials Characterizations

TCPP (Figure 1A), a water-soluble anion porphyrin that can strongly adsorb on graphene (Figure 1B)through stacking and hydrophobic interactions, which could be used to avoid graphene aggregation and introduce more negatively-charged –COOH groups on graphene surface, without further destroying the conjugated system of graphene [24-26]. TEM (Figure 1C) shows that TCPP/RGO surface has a thin wrinkling paperlike structure.

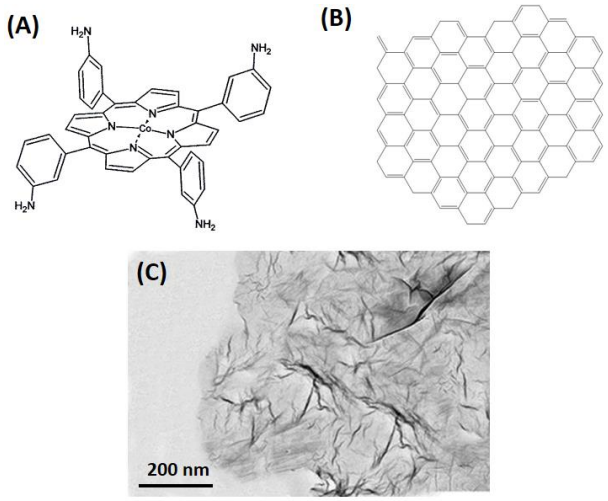

Figure 1. The structure of (A) TCPP and (B) graphene. (C) TEM image of the prepared TCPP-RGO.

3.2. Electrochemical Characterizations

From Figure 2A, it can be seen that the cyclic voltammetry (CV) is used by electrochemical activities of various materials modified GC electrodes for characterizing toward $Fe(CN)_6^{3-/4-}$. Compared with that of the porphyrin improved GC electrode, the CVs indicate that in terms of the TCPP-RGO modified GC electrode, the electrochemical redox reaction of $Fe(CN)_6^{3-/4-}$ has higher peak current and more symmetric peaks, which shows that for the bigger current toward $Fe(CN)_6^{3-/4-}$. The grapheme/porphyrin that boosted GC electrode has superior electrocatalytic activity for the larger reaction area and more reversible reactions. Based on the Randles–Sevcik equation [27, 28], ip = $2:99\times10^5$ $nACD^{1/2}v^{1/2}$, estimation of surface area of electroactivity can be done. The v, D, C, A, n, Ip are the scan rate, the diffusion coefficient of the reactant species, reactant concentration, surface area of electroactivity, quantity of electrons in the reaction, the electroactive surface area, and peak current, respectively. Diffusion coefficient (D) is 6.30×10^{-6} cm^2/s, and in the redox reaction of $Fe(CN)_6^{3-/4-}$, one-electron transfer (n=1) is involved. The rate of A for grapheme/porphyrin improved GC electrode (7.3×10^{-2} cm^2) is three times bigger than that of porphyrin modified GC electrode (3.4×10^{-2} cm^2), and two times bigger than that of bare GC electrode (4.1×10^{-2} cm^2), which show that for bigger apparent current density, incorporating the graphene can greatly boost the reaction surface area of electrode.

Compared with the surface area of graphene modified GC electrode of 12.8×10^{-2} cm^2, the TCPP-RGO modified GC electrode surface area of 11.3×10^{-2} cm^2 is smaller. The result shows that the although catalysis of porphyrin is alternative, it can greatly promote several particular electrochemical reactions like the reduction of oxygen [29], but not toward redox reaction of $Fe(CN)_6^{3-/4-}$.

Electrochemical impedance spectroscopy (EIS) was applied for the deeper study of the electrochemical electrodes behaviors. The Figure 2B shows the results. For modeling the complex impedance of an electrochemical cell, commonly randle equivalent circuit is applied [30, 31]. The equivalent circuit consists of Z_f (Faraday impedance) and R_s (the resistance of the electrolyte), continuously connecting with parallel elements of Cdl (double layer capacitance). Commonly, Z_f comprises serially connected R_{ct} (charge-transfer resistance), which decides Z w (Warburg impedance) and the diameter of the semicircle. By being calculated from randle equivalent circuit for TCPP-RGO modified GC electrode, compared with the rate of porphyrin modified GC electrode of 621 Ω, R_{ct} (297 Ω) rate is greatly lower, which shows that in the TCPP-RGO the graphene can boost rapid charge transfer rate. The impedance Z is as same as the square root of sum of square of imaginary part. In addition, the square of real part (R_s+Z_f) that object to the frequency is found. When the frequency grows into a bigger rate, in fact, the real part of the impedance rate is nearly constant to correspond to the electrode resistivity and is the DC resistance. The inset of Figure 3B indicates that compared with the rate of porphyrin modified GC electrode, the rate of the TCPP-RGO modified GC electrode is much lower, which shows better conductivity of porphyrin/graphene modified GC electrode. Nevertheless, compared with R_{ct} of bare GC electrode (125 Ω), R_{ct} (178 Ω) calculated for the porphyrin/graphene modified GC electrode is bigger, consistent with its peak potential separation, which is bigger than that of bare GC electrode, further presenting that porphyrin catalysis is greatly alternative and do not improve electron transfer for $Fe(CN)_6^{3-/4-}$ reaction.

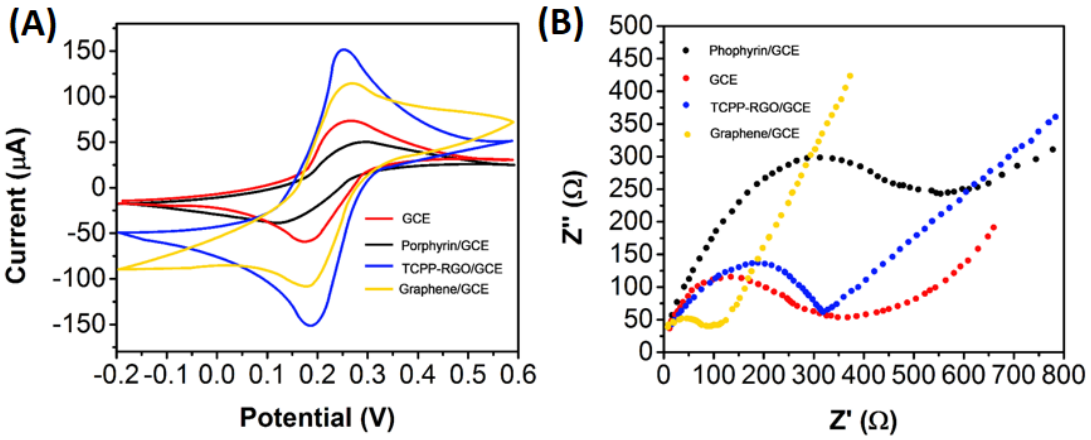

Figure 2. (A) Cyclic voltammograms (CVs) and (B) Electrochemical impedance spectroscopy (EIS) spectra of 10 mM $Fe(CN)_6^{3-/4-}$ in 1.0 M KCl at bare GCE, TPCC modified GC electrode, porphyrin modified GC electrode and TCPP-RGO modified GC electrode. Scan rate: 50 mV/s.

Electrochemistry characterization can provides the more information of forming the TCPP-RGO hybrid nanosheets. It can be shown in Figure 3A, the TCPP-RGO modified GC electrode at various scan rates in PBS (pH7.4) solution show classic CVs profile. Because of oxidation/reduction of porphyrin, redox wave was detected in −0.25 V formal potential. In the same electrolyte, compared with the original porphyrin modified GC, the redox potential (62 mV) of TCPP-RGO is more negative, which maybe because that on the attachment of the porphyrin on RGO surface, which service as redox centers. The electron-drawing effect causes the negative potential shift. The TCPP-RGO indicates great redox reversibility and its peak-to-peak separation was approximate 32 mV. Because of the famous interpenetration phenomenon within the GO surface that allows an electron hopping process between adjacent redox groups, it can be shown from results that porphyrin molecules may contact with each other electrically. Compared with redox potential of porphyrin/GC redox, the potential of TCPP-RGO modified GC electrode is larger, which indicates that the interactions between RGO and porphyrin promote electron to transfer from modifier to surface of electrode. For the TCPP-RGO nanosheets, in aqueous solution, the reversibility of the voltammetric reactions is greatly boosted, when in comparison with those of other porphyrin nanomaterials [32-34].

The TCPP-RGO modified GC electrode indicates the feature that redox electrochemistry has the surface that is chemically reversible. In the inset of Figure 3B, as a function of scan rate, the plot of the cathodic peak current is a linear corresponding to the scan rates reach to 800 mV/s. In addition, the formal potentials are excluding the scan rates, and at all scan rates, the currents ratios of anodic peak and cathodic peak are unity. It can be shown that the surface of redox processes is confined by porphyrin, from the underlying substrate to TCPP-RGO modified GC, which is quick. Based on these results, the average surface coverage of the porphyrin molecule on RGO surface is 0.66095 $\times 10^{-7}$ mol/g. Additionally, during the whole electrochemical examination, it is found that the TCPP-RGO modified GC electrode be overly steady by cycling in −0.6 and 0.2 V for 1 h, indicating the excellent stability, which make commercial electrochemical catalysis become possible.

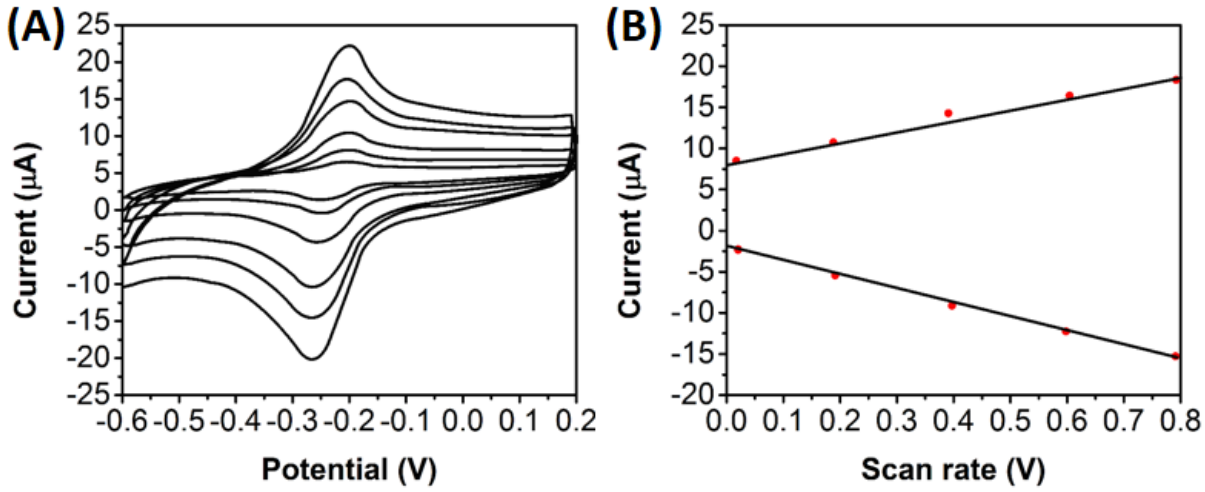

Figure 3. (A) Voltammetric response of the TCPP-RGO modified GC electrode in PBS (0.1M, pH 7.4) at scan rate from 10mV/s to 800 mV/s. Scan rate: 50 mV/s. (B) Plots of dependence of peak currents on scan rates for the TCPP-RGO modified GC electrode.

It is showed in Figure 4 that when various amounts of UA at an applied potential 0.25 V are investigated, the responses could reach to stable state within 5 s. The quick response suggesting that the electrode reaction to towards UA is rapid. The fast reaction would be mainly ascribed to two reasons. The first reason is the synergistic catalytic effect in the TCPP-RGO nanosheets toward UA. The second reason is, in the TCPP-RGO hybrid nanosheets on the electrode, the UA diffusion is rapid. The response shows a great linear range from 0.02 to 5 mM and detection limit is 1 μM.

In comparison of literature reports, the detection limit of our proposed sensor is lower than that obtained at a surfactant–clay modified GCE [35]. The linear response range of our proposed sensor is wider than those of 10 μM–2.64 mM at poly (acid chrome blue K) modified glassy carbon electrode and 5 μM–1.5 mM at single-walled carbon nanohorn modified glassy carbon electrode [36]. The detail comparison was summarized in Table 1. The UA concentrations in serum and urinary excretion are commonly in the range of 0.3 to 0.5 mM and 1.4–4.4 mM, respectively. Therefore, based on our results, the proposed TCPP-RGO modified electrode could potentially determining UA content in serum and urinary excretion.

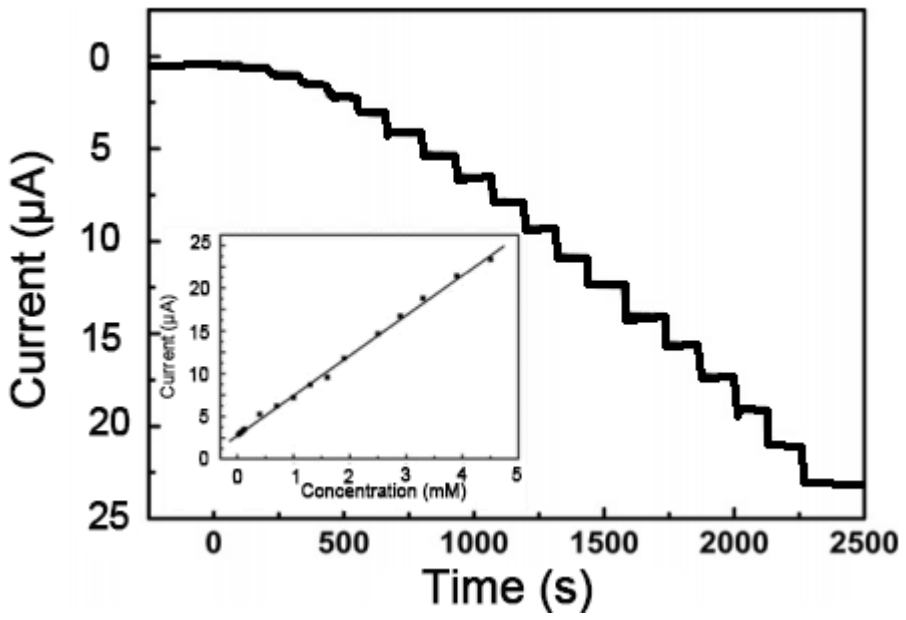

Figure 4. The electrochemical current responses of a proposed TCPP-RGO electrochemical UA sensor with success addition of UA (detection potential: 0.25V). Inset: calibration curve UV concentrations and current responses.

Table 1. Comparison of proposed UA electrochemical sensor with other reports.

Electrode	LDR (μM)	LOD (μM)	Reference
Au/RGO/GCE	8.8-530	0.18	[37]
Palladium nanoparticle/graphene/chitosan	1-200	0.17	[38]
Reduced graphene oxide	0.5–60	0.02	[39]
Graphene-modified carbon fiber	0.194-49.68	0.132	[40]
Nitrogen doped graphene	0.1-200	0.045	[41]
TCPP-RGO	20–5000	1	This work

The stability and reproducibility of the biosensor were assessed. In the present response to 2 mM UA, six various TCPP-RGO modified GC electrodes were studied. The results showed that the biosensor was of excellent reproducibility and a relevant standard deviation (RSD) of 3.6%. Additionally, 10 various amperometric examinations for 2 mM UA at 0.25 V with sole biosensor produced recorded a RSD of 2.6%, which showed great repeatability of the examinations.

In practical analysis, the TCPP-RGO modified GC electrode was applied for measurement of UV in blood and urine samples. Firstly, spectrophotometric method would be used to analyze the urine samples and fresh human blood. Secondly, biosensor would be employed for examining the samples. At 0.25 V, with the additional 0.2 ml sample was added into 5 ml PBS, a reliable and fast amperometric response was obtained. From the calibration curve, the UV content in urine and blood can be calculated. Table 2 shows the determination result. The excellent recoveries indicated that the TCPP-RGO modified GC electrode could successful determination of UA in real samples.

Table 2. Determination of UA in human blood and urine samples using spectrophotometric method and proposed electrochemical sensor.

Sample	Spectrophotometric determination	RSD (%)	Recovery (%)	TCPP-RGO/GCE	RSD (%)	Recovery (%)
Blood	0.23	4.85	97.21	0.22	2.95	98.6
	0.45	5.55	98.69	0.46	2.63	99.3
Urine	3.51	7.51	104.21	3.54	3.51	100.2
	4.25	2.98	89.66	4.21	1.23	99.5
	2.61	3.69	90.24	2.58	5.11	101.3

4. CONCLUSION

To quickly prepare the TCPP-RGO hybrid nanosheets, a wet-chemical method was presented. In terms of the simplicity, the method proposed was special. The consequential TCPP-RGO was adopted as progressive electrode materials and broadly studied through different kinds of characterization methods, which included TEM and AFM. The neo-composite material combined electronic properties of RGO and special and fascinating electrocatalytic behavior of porphyrin with good biocompatible. Based on these special properties of the new material, a new method for measurement was created UA. The biosensor showed a wide linear range, a quick response, a low level of detecting limitation with excellent repeatability and stability. At the same time, in terms of UA measurement, the biosensor is of important potential application. The large surface area of RGO makes great contribution to these valuable biosensor performances, which is good for good biocompatibility, high conductivity, and quick mass transport as well as the synergistic catalytic effect between porphyrin and RGO. The production method of the biosensor possesses numerous merits, including strengthened electrocatalysis and ease of fabrication.

ACKNOWLEDGEMENTS
This work was funded by National Training Programs of Innovation and Entrepreneurship for Undergraduates (201610069037); Tianjin Key Laboratory for Prevention and Control of Occupational and Environmental hazards Opening Fund (WHKF201504).

References

1. U.M. Khosla, S. Zharikov, J.L. Finch, T. Nakagawa, C. Roncal, W. Mu, K. Krotova, E.R. Block, S. Prabhakar and R.J. Johnson, *Kidney international*, 67 (2005) 1739
2. J.F. Baker, E. Krishnan, L. Chen and H.R. Schumacher, *The American journal of medicine*, 118 (2005) 816
3. J. Bowen, L. Chamley, M. Mitchell and J. Keelan, *Placenta*, 23 (2002) 239
4. H.L. Zou, B.L. Li, H.Q. Luo and N.B. Li, *Sensors and Actuators B: Chemical*, 207 (2015) 535
5. S. Qi, B. Zhao, H. Tang and X. Jiang, *Electrochimica Acta*, 161 (2015) 395
6. A. Benvidi, A. Dehghani-Firouzabadi, M. Mazloum-Ardakani, B.-B.F. Mirjalili and R. Zare, *Journal of Electroanalytical Chemistry*, 736 (2015) 22
7. Y. Liu, P. She, J. Gong, W. Wu, S. Xu, J. Li, K. Zhao and A. Deng, *Sensors and Actuators B: Chemical*, 221 (2015) 1542
8. H. Zhou, W. Wang, P. Li, Y. Yu and L. Lu, *Int. J. Electrochem. Sci*, 11 (2016) 5197
9. B. Kaur, B. Satpati and R. Srivastava, *New J Chem*, 39 (2015) 1115
10. L. Fritea, M. Tertiş, C. Cristea, S. Cosnier and R. Săndulescu, *Analytical Letters*, 48 (2015) 89
11. A. Rajamani, R. Kannan, S. Krishnan, S. Ramakrishnan, S.M. Raj, D. Kumaresan, N. Kothurkar and M. Rangarajan, *Journal of nanoscience and nanotechnology*, 15 (2015) 5042
12. L. Fu, G. Lai, G. Chen, C.T. Lin and A. Yu, *ChemistrySelect*, 1 (2016) 1799
13. Y. Zheng, Z. Wang, F. Peng, A. Wang, X. Cai and L. Fu, *Fullerenes, Nanotubes and Carbon Nanostructures*, 24 (2016) 149
14. L. Fu, S. Yu, L. Thompson and A. Yu, *RSC Advances*, 5 (2015) 40111
15. L. Fu, G. Lai and A. Yu, *RSC Advances*, 5 (2015) 76973
16. D.M. Guldi and M. Prato, *Accounts of chemical research*, 33 (2000) 695
17. R.B. Martin, H. Li, L. Gu, S. Kumar, C.M. Sanders and Y.-P. Sun, *Optical Materials*, 27 (2005) 1340
18. D.M. Guldi, G.A. Rahman, V. Sgobba and C. Ehli, *Chemical Society Reviews*, 35 (2006) 471
19. Y. Xu, L. Zhao, H. Bai, W. Hong, C. Li and G. Shi, *Journal of the American Chemical Society*, 131 (2009) 13490
20. Y. Guo, L. Deng, J. Li, S. Guo, E. Wang and S. Dong, *ACS nano*, 5 (2011) 1282
21. S. Tao, G. Li and J. Yin, *Journal of Materials Chemistry*, 17 (2007) 2730
22. S. Tao, G. Li and H. Zhu, *Journal of Materials Chemistry*, 16 (2006) 4521
23. X. Wang, S.M. Tabakman and H. Dai, *Journal of the American Chemical Society*, 130 (2008) 8152
24. A. Ghosh, K.V. Rao, S.J. George and C. Rao, *Chemistry–A European Journal*, 16 (2010) 2700
25. D. Li, M.B. Mueller, S. Gilje, R.B. Kaner and G.G. Wallace, *Nature nanotechnology*, 3 (2008) 101
26. W. Tu, J. Lei, S. Zhang and H. Ju, *Chemistry–A European Journal*, 16 (2010) 10771
27. C. Guo, F. Hu, C.M. Li and P.K. Shen, *Biosensors and Bioelectronics*, 24 (2008) 819
28. S. Biswas and L.T. Drzal, *Chemistry of Materials*, 22 (2010) 5667
29. Q. Zhou, C.M. Li, J. Li, X. Cui and D. Gervasio, *J Phys Chem C*, 111 (2007) 11216
30. W. Sun, C.X. Guo, Z. Zhu and C.M. Li, *Electrochemistry communications*, 11 (2009) 2105
31. C.X. Guo, F.P. Hu, X.W. Lou and C.M. Li, *Journal of Power Sources*, 195 (2010) 4090
32. F. Song, J. Jia, J. Yu, C. Chen, J. Feng and P. Zhu, *Inorganic Chemistry Communications*, 61

(2015) 149
33. S. Kazemi, B. Hosseinzadeh and S. Zakavi, *Sensors and Actuators B: Chemical*, 210 (2015) 343
34. S. Munir, S.M. Shah, H. Hussain and M. Siddiq, *J. Photoch. Photobio. B*, 153 (2015) 397
35. L. Fernández and H. Carrero, *Electrochimica Acta*, 50 (2005) 1233
36. S. Zhu, H. Li, W. Niu and G. Xu, *Biosensors and Bioelectronics*, 25 (2009) 940
37. C. Wang, J. Du, H. Wang, C.e. Zou, F. Jiang, P. Yang and Y. Du, *Sensors and Actuators B: Chemical*, 204 (2014) 302
38. X. Wang, M. Wu, W. Tang, Y. Zhu, L. Wang, Q. Wang, P. He and Y. Fang, *Journal of Electroanalytical Chemistry*, 695 (2013) 10
39. L. Yang, D. Liu, J. Huang and T. You, *Sensors and Actuators B: Chemical*, 193 (2014) 166
40. J. Du, R. Yue, Z. Yao, F. Jiang, Y. Du, P. Yang and C. Wang, *Colloids and Surfaces A: Physicochemical and Engineering Aspects*, 419 (2013) 94
41. Z.-H. Sheng, X.-Q. Zheng, J.-Y. Xu, W.-J. Bao, F.-B. Wang and X.-H. Xia, *Biosensors and Bioelectronics*, 34 (2012) 125